



HAL
open science

Switching control applied to interconnected Boost converters: A comparison with hysteresis current control

Ryan P C de Souza, Zohra Kader, Stéphane Caux

► **To cite this version:**

Ryan P C de Souza, Zohra Kader, Stéphane Caux. Switching control applied to interconnected Boost converters: A comparison with hysteresis current control. 26th International Symposium on Power Electronics, Electrical Drives, Automation and Motion (SPEEDAM), Jun 2022, Sorrento, Italy. 10.1109/SPEEDAM53979.2022.9842143 . hal-03683641

HAL Id: hal-03683641

<https://hal.science/hal-03683641v1>

Submitted on 6 Jun 2023

HAL is a multi-disciplinary open access archive for the deposit and dissemination of scientific research documents, whether they are published or not. The documents may come from teaching and research institutions in France or abroad, or from public or private research centers.

L'archive ouverte pluridisciplinaire **HAL**, est destinée au dépôt et à la diffusion de documents scientifiques de niveau recherche, publiés ou non, émanant des établissements d'enseignement et de recherche français ou étrangers, des laboratoires publics ou privés.

Switching control applied to interconnected Boost converters: A comparison with hysteresis current control

Ryan P. C. de Souza, Zohra Kader, *Member, IEEE*, and Stéphane Caux, *Member, IEEE*

Abstract—In this paper, the stabilization of the voltage at the output of Boost converters is studied using a switching control method developed in the field of switched affine systems. This control law uses the instantaneous model instead of the nonlinear average model of the converter and has certain advantages compared to traditional approaches. Despite these advantages, the closed-loop system suffers from the occurrence of sliding modes, leading to unacceptable rises in the switching frequency. An adaptation of this control law is proposed in this paper to overcome this problem, and the adopted strategy is based on the introduction of hysteresis in the switching law. Moreover, the extension to Boost converters in parallel is also shown, with the attractive property of each converter only needing local measurements for global stabilization of the system. A comparison with the hysteresis current control method is conducted in simulations.

I. INTRODUCTION

Due to the objectives of mitigating the rise in greenhouse gas emissions in electricity generation, there has been a growing demand for renewable sources. Depending on the application, they can be integrated in a DC microgrid, which is a solution that is increasingly popular due to a number of reasons, including higher efficiency and a more natural interface with many types of renewable sources [1].

In some scenarios, the energy sources connected to a microgrid produce a lower voltage compared with the voltage at the DC bus. This is often the case with photovoltaic panels [2]. In this case, Boost converters are suitable for interfacing the sources with the microgrid [3]. This raises the question of how to control each converter in order to stabilize the main bus at the desired voltage reference.

In order to tackle the challenge of global stabilization of the DC microgrid, a switching control law introduced in [4] is used in this paper. This control method is based on the instantaneous model of the converters, instead of the more traditional approach of using their (often nonlinear) average models. Moreover, the switching law can be deduced by solving a Linear Matrix Inequality (LMI), for which efficient solvers are available. Two advantages of this method are: (i) Pulse-Width Modulation (PWM) is not required to generate the gate signal to each switching device, since the control law can already provide it, and (ii) linearization of the model is not necessary (as it is normally the case when working with Boost converters, whose average models are nonlinear) and global stabilization can be theoretically ensured. The main issue with the control method in [4] is that it leads

to sliding modes (with ideally infinite-rate switching), and thus the switching frequency rises to unacceptable values, damaging the switches.

The aim of this paper is to overcome the issue of infinite switching frequency by employing hysteresis. In addition, the proposed hysteresis-based switching method applies only local measurements, meaning that the resulting control law is decentralized. This can be interesting in practical situations where communication between different source units is impaired or non-existent.

This paper is organized as follows. In Section II, the instantaneous models of the two systems addressed here are presented. In Section III, the method proposed in this paper is introduced for both systems presented in Section II. Simulation results comparing the proposed method with hysteresis current control are shown in Section IV. Finally, conclusions are drawn in Section V.

Notation: If w is a vector, then $w_{(k)}$ denoted its k -th component. If Q is a matrix, Q^T is its transpose, and $Q \prec 0$ (resp. $Q \succ 0$) means that Q is negative-definite (resp. positive-definite). The null matrix of q rows and r columns is denoted as $0_{q \times r}$. Given a positive integer N , the unit simplex Δ_N is defined as $\Delta_N := \{\delta \in [0, 1]^N : \sum_{k=1}^N \delta_{(k)} = 1\}$ and set \mathcal{I}_N is defined as $\mathcal{I}_N := \{1, 2, \dots, N\}$. Given matrices Q_k , $k = 1, 2, \dots, N$, their convex combination defined by $\delta \in \Delta_N$ is denoted as $Q(\delta) := \sum_{k=1}^N \delta_{(k)} Q_k$.

II. SYSTEM MODELS

In this section, the mathematical models of the two converter configurations addressed in this paper are presented. It is assumed that the converters always operate in continuous current mode. First, consider the equation describing the dynamics of a *switched affine system* [4], [5], [6]:

$$\dot{z}(t) = A_\sigma z(t) + B_\sigma, \quad (1)$$

where σ is a discrete variable taking values in the set \mathcal{I}_M , with M denoting the number of modes in the system. Vector z is the state vector, and matrices A_σ and B_σ , $\sigma = 1, \dots, M$, are the system parameters. At each time instant, the system evolves according to the dynamics dictated by one of the modes, and the system can always switch from one mode to another at any time.

A. Single Boost converter

Consider the idealized circuit of the Boost converter depicted in Fig. 1. Let $i(t)$ be the current flowing in inductor L (i.e., the input current) and $v(t)$ be the output voltage.

The authors are with LAPLACE - Université de Toulouse, 118 route de Narbonne 31062 Toulouse cedex 9, France {pitanga,kader,caux}@laplace.univ-tlse.fr

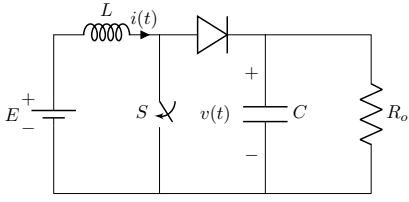


Fig. 1: Boost converter supplying a load R_o .

Since in this paper the instantaneous model is considered, the model is determined from the current and voltage laws applied to the circuit according to whether switch S is closed or not. By introducing the discrete variable $\sigma \in \mathcal{I}_2$, with $\sigma = 1$ corresponding to the situation where S is closed and $\sigma = 2$ to when S is open, the equation governing the system dynamics is given by (1), with state $z(t)$ being equal to $z(t) = [i(t) \ v(t)]^T$ in this case and with:

$$A_1 = \begin{bmatrix} 0 & 0 \\ 0 & -1/(R_o C) \end{bmatrix}, \quad B_1 = \begin{bmatrix} E/L \\ 0 \end{bmatrix}, \quad (2)$$

$$A_2 = \begin{bmatrix} 0 & -1/L \\ 1/C & -1/(R_o C) \end{bmatrix}, \quad B_2 = B_1. \quad (3)$$

Note that the number of modes is $M = 2$. Define i^* and v^* as the input current and the output voltage in equilibrium, respectively. The equilibrium points of (1) can be determined using the formalism of discontinuous systems (see, for instance, [7]). Using this formalism, $z^* = [i^* \ v^*]^T$ is an equilibrium of (1) if there exists $\delta^* \in \Delta_M$ such that:

$$\sum_{\sigma=1}^M \delta_{(\sigma)}^* (A_{\sigma} z^* + B_{\sigma}) = 0, \quad (4)$$

Let $\alpha^* := \delta_{(1)}^* \in [0, 1]$. Since $\delta_{(2)}^* = 1 - \alpha^*$, then (4) can be written as:

$$\alpha^* (A_1 z^* + B_1) + (1 - \alpha^*) (A_2 z^* + B_2) = 0. \quad (5)$$

Note that (5) is exactly the same equation of the state-space average dynamics [8] in equilibrium, wherein α^* corresponds to the duty cycle in steady state. Therefore, the equilibrium of the instantaneous model (1) can be characterized in the same way as in the case of the nonlinear average model. From (5), one can easily obtain the classical relationship between the input and steady-state output voltages:

$$v^* = \frac{E}{1 - \alpha^*}. \quad (6)$$

The inductor current reference i^* can be calculated as:

$$i^* = \frac{v^*}{(1 - \alpha^*) R_o}. \quad (7)$$

It is also useful to define the *dynamics in equilibrium in mode* σ as $b_{\sigma} := A_{\sigma} z^* + B_{\sigma}$, $\sigma = 1, 2$.

B. Boost converters in parallel

In Fig. 2, the connection of two Boost converters feeding a load is shown. Each one is connected to the load through an LC filter modeled by capacitance C_j and inductance L'_j , $j \in \{1, 2\}$. Note that the parasitic resistances associated with this inductor is represented by R'_j . Parameters L'_j and R'_j

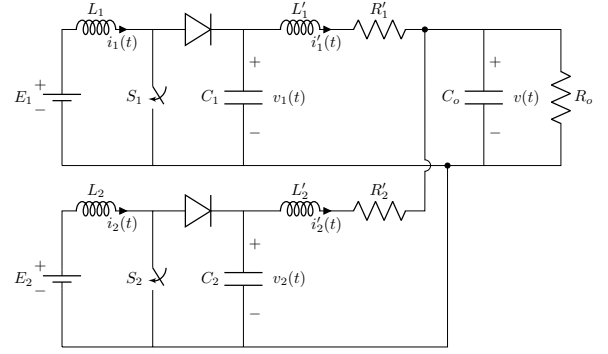


Fig. 2: Two Boost converters supplying load R_o .

TABLE I: States of the switches in each mode $\sigma \in \{1, 2, 3, 4\}$.

σ	σ_1	σ_2
1	1	1
2	1	2
3	2	2
4	2	1

could also be used to model the inductance and the resistance of the cables connecting each converter to the DC bus, to which the load R_o is connected. The capacitance of the bus is modeled by C_o .

The state vector, for this system, is given by $z(t) = [z_1(t)^T \ z_2(t)^T \ v(t)]^T$, where $z_j(t) = [i_j(t) \ v_j(t) \ i'_j(t)]^T$ represents the local state variables of the j -th converter, $j = 1, 2$. Note that the output current of each converter (i'_j) has been included as a local variable.

Since two switches are present in the circuit, σ can take 4 different values, each one corresponding to a different combination of switches S_1 and S_2 . Thus, the number of modes is $M = 4$. Table I shows the state of each switch σ_j , $j = 1, 2$, for each mode $\sigma \in \mathcal{I}_4$. The convention adopted here is that $\sigma_j = 1$ when S_j is closed and $\sigma_j = 2$ when it is open.

Using the circuit laws once again for each different mode, the dynamics are dictated by (1), and are written here as¹:

$$\dot{z} = \begin{bmatrix} \dot{z}_1 \\ \dot{z}_2 \\ \dot{v} \end{bmatrix} = \begin{bmatrix} g_{1,\sigma_1}(z_1, v) \\ g_{2,\sigma_2}(z_2, v) \\ \dot{v} \end{bmatrix} = A_{\sigma} z + B_{\sigma}, \quad (8)$$

with $g_{j,\sigma_j}(z_j, v)$ defined as the dynamics of the local variables of converter j , and matrices A_{σ} and B_{σ} , $\sigma = 1, \dots, 4$, are in this case given by:

$$A_1 = \begin{bmatrix} \begin{array}{c|c|c} A_{1,1} & 0_{3 \times 3} & W \\ \hline 0_{3 \times 3} & A_{2,1} & \\ \hline \hline \hline \end{array} & a_o \end{bmatrix}, \quad (9)$$

$$A_2 = \begin{bmatrix} \begin{array}{c|c|c} A_{1,1} & 0_{3 \times 3} & W \\ \hline 0_{3 \times 3} & A_{2,2} & \\ \hline \hline \hline \end{array} & a_o \end{bmatrix}, \quad (10)$$

$$A_3 = \begin{bmatrix} \begin{array}{c|c|c} A_{1,2} & 0_{3 \times 3} & W \\ \hline 0_{3 \times 3} & A_{2,2} & \\ \hline \hline \hline \end{array} & a_o \end{bmatrix}, \quad (11)$$

¹ σ_1 and σ_2 are associated with mode σ according to Table I.

$$A_4 = \begin{bmatrix} \begin{array}{c|c|c} A_{1,2} & 0_{3 \times 3} & W \\ \hline 0_{3 \times 3} & A_{2,1} & \\ \hline & U & a_o \end{array} \end{bmatrix}, \quad (12)$$

and

$$B_1 = B_2 = B_3 = B_4 = \begin{bmatrix} E_1/L_1 \\ 0_{2 \times 1} \\ \bar{E}_2/\bar{L}_2 \\ 0_{2 \times 1} \\ 0 \end{bmatrix}, \quad (13)$$

where:

$$A_{j,1} := \begin{bmatrix} 0 & 0 & 0 \\ 0 & 0 & -1/C_j \\ 0 & 1/L'_j & -R'_j/L'_j \end{bmatrix}, \quad j = 1, 2, \quad (14)$$

$$A_{j,2} := \begin{bmatrix} 0 & -1/L_j & 0 \\ 1/C_j & 0 & -1/C_j \\ 0 & 1/L'_j & -R'_j/L'_j \end{bmatrix}, \quad j = 1, 2, \quad (15)$$

$$W := [0 \ 0 \ -1/L'_1 \ 0 \ 0 \ -1/L'_2]^T, \quad (16)$$

$$U := [0 \ 0 \ 1/C_o \ 0 \ 0 \ 1/C_o], \quad (17)$$

and

$$a_o := -\frac{1}{R_o C_o}. \quad (18)$$

By using once again the formalism of discontinuous systems, the equilibrium points z^* satisfy (4), with $M = 4$. Let $\alpha_1^* := \delta_{(1)}^* + \delta_{(2)}^*$ and $\alpha_2^* := \delta_{(1)}^* + \delta_{(4)}^*$ denote the duty cycles of converters 1 and 2, respectively. Then, the equilibrium points z^* satisfy the following relations:

$$v_j^* = \frac{E_j}{1 - \alpha_j^*}, \quad j = 1, 2, \quad (19)$$

$$i_j^* = (1 - \alpha_j^*)i_j^*, \quad j = 1, 2, \quad (20)$$

$$v_j^* = v^* + R'_j i_j^*, \quad j = 1, 2, \quad (21)$$

$$v^* = R_o(i_1^* + i_2^*). \quad (22)$$

There is a certain freedom with respect to how the load current is shared between the output currents of both converters. For the purposes of this paper, it is simply assumed that $i_2^* = \kappa i_1^*$, where $\kappa \geq 0$ is a design parameter. Thus, (22) becomes:

$$i_1^* = \frac{v^*}{R_o(\kappa + 1)}. \quad (23)$$

The dynamics in equilibrium for each mode of converter j is simply defined as $b_{j,\sigma_j} := g_{j,\sigma_j}(z_j^*, v^*)$, $\sigma_j = 1, 2$, $j = 1, 2$.

Remark 1: It can be seen that the modeling procedure for the converters in parallel is modular, in the sense that the parameter matrices can be algorithmically constructed from blocks corresponding to each module. This makes the modeling process scalable to a large number of converters in parallel, as in the case of a DC microgrid. Note also that more complex configurations for linear output filters can be considered through proper choices for matrices $A_{j,1}$, $A_{j,2}$, $j = 1, 2$, and W . This means that the control law discussed in the next two sections may be used in more complex scenarios. \square

III. HYSTERESIS-BASED SWITCHING CONTROL

A. Ideal switching law for switched affine systems

The switching law presented in the sequel has been proposed in [4] for global stabilization of switched affine systems. Firstly, assume that the following LMI is feasible:

$$A(\delta^*)^T P + P A(\delta^*) \prec 0, \quad (24)$$

for some $P = P^T \succ 0$. Vector δ^* is obtained according to the desired equilibrium point. For example, in the case of a single Boost converter, $\delta^* = [\alpha^* \ 1 - \alpha^*]^T$ and α^* is the duty cycle determined from (5) to obtain the desired steady-state output voltage v^* .

With a matrix P satisfying (24), the following control law exponentially stabilizes system (1) at z^* [4]:

$$\sigma(z) \in \arg \min_{m \in \mathcal{I}_M} (z - z^*)^T P (A_m z + B_m). \quad (25)$$

In the system models used in this paper, $B_1 = B_2 = \dots = B_M$. With this in mind, (25) can be simply written as:

$$\sigma(z) \in \arg \min_{m \in \mathcal{I}_M} (z - z^*)^T P A_m z. \quad (26)$$

Since $\sigma(z)$ only depends on z , it is said that (26) is a state-dependent control law. It is interesting to remark that the application of control law (26) does not require the system to be linearized around the desired equilibrium point. And yet, as shown in [4], the equilibrium point is globally exponentially stable. This contrasts with the use of more traditional methods, where linearization of the average model is employed and thus stability can only be ensured in a neighborhood of the equilibrium. Moreover, since (26) directly selects the mode that should be activated, a PWM module generating the gate signal for the switching device is not needed.

B. Adding hysteresis

The main drawback of the switching strategy described by (26) is that it leads to sliding modes [4]. Thus, direct application of (26) causes the switching frequency to rise to unacceptable levels, possibly damaging the switching devices. The proposed method for overcoming this issue is based on an adaptation of control law (26) to incorporate hysteresis and the development of this method is carried out for the particular cases of the two systems presented in Section II. The newly obtained control shall be referred to as *Hysteresis-Based Switching Control* (HBSC).

1) *Single Boost converter:* In the case of one Boost converter, there are only two modes. Define $s(z) := (z - z^*)^T P D z$, where $D := A_1 - A_2$. The application of (26) implies the following:

- $\sigma(z) = 1$, if $s(z) < 0$;
- $\sigma(z) = 2$, if $s(z) > 0$;
- $\sigma(z) \in \{1, 2\}$ if $s(z) = 0$.

On the *switching surface* $s(z) = 0$, there are two possibilities for the evolution of the system trajectory: (i) the mode is switched from one to the other and the trajectory simply crosses the surface to the other side; (ii) a sliding mode occurs along the switching surface.

The HBSC can be described as follows: instead of switching as soon as the trajectory reaches the switching surface, switching is stopped while $|s(z)| < h$, where $h > 0$ is a design parameter. When $|s(z)| \geq h$, then the mode is chosen according to (26). In the sequel, the link between h and the steady-state switching frequency is made clear.

Due to hysteresis, the behavior of the system in steady state is characterized by periodical oscillations in the current and voltage. Just as in traditional methods in power electronics, the system spends a certain time t_1 in mode 1 and a time t_2 in mode 2. The sum of t_1 and t_2 gives the switching period, whose inverse is the switching frequency f_{ss} .

It is assumed that h is sufficiently small so that the time evolution of $s(z)$ is piecewise linear. This assumption is analogous to the statement often made in power electronics that the switching frequency is very high with respect to the bandwidth of the system. Thus, in order to keep the current or voltage ripples at acceptable levels, this assumption often holds in practice. Since, during hysteresis, $s(z)$ varies between $-h$ and h (and thus the absolute variation of $s(z)$ is $2h$):

$$|\dot{s}(z)| = \frac{2h}{t_\sigma}, \quad \sigma = 1, 2, \quad (27)$$

for z in a small neighborhood of z^* . The gradient of $s(z)$ is given by:

$$\nabla s(z) = (D^T P + PD)z - D^T P z^*. \quad (28)$$

In the neighborhood of z^* , $\dot{s}(z)$ can be approximated by $\dot{s}(z^*) = \nabla s(z^*)^T b_\sigma$ while in mode σ . Since $\nabla s(z^*) = PDz^*$, the following expressions are obtained from (27):

$$t_\sigma = \frac{2h}{|z^{*T} D^T P b_\sigma|}, \quad \sigma = 1, 2. \quad (29)$$

From (29) and the fact that f_{ss} is the inverse of the sum of t_1 and t_2 , the following expression is obtained:

$$f_{ss} = \frac{1}{2h} \frac{|b_1^T PDz^* z^{*T} D^T P b_2|}{(|b_1^T PDz^*| + |b_2^T PDz^*|)}. \quad (30)$$

The acceptable current ripple ΔI is linked to the switching frequency by the same expression that is normally used in traditional methods:

$$\Delta I = \frac{\alpha^* E}{L f_{ss}}. \quad (31)$$

Thus, from (30) and (31), h can be determined to bound the current ripple at a value ΔI chosen by the designer.

2) *Boost converters in parallel:* In the case of the Boost converters in parallel, there are 4 modes instead of 2. This means that there are more than one switching surface, and each one may involve all state variables of the system. However, a procedure is proposed in the sequel to implement hysteresis separately in each converter, where only local measurements are used in the control law. As it will be seen, only one switching surface may be considered for each converter, and thus hysteresis may be implemented in a similar way as for a single converter. Firstly, rewrite matrices

A_σ and B_σ , $\forall \sigma \in \mathcal{I}_4$, as follows:

$$A_\sigma = \begin{bmatrix} \overbrace{0_{6 \times 6} \quad W}^{\bar{A}} \\ U \quad a_o \end{bmatrix} + \begin{bmatrix} \overbrace{A_{1,\sigma_1} \quad 0_{3 \times 4}}^{\bar{A}_{1,\sigma_1}} \\ \overbrace{0_{4 \times 3} \quad 0_{4 \times 4}}^{\bar{A}_{1,\sigma_1}} \end{bmatrix} + \begin{bmatrix} 0_{3 \times 3} & 0_{3 \times 3} & 0_{3 \times 1} \\ 0_{3 \times 3} & A_{2,\sigma_2} & 0_{3 \times 1} \\ 0_{1 \times 3} & 0_{1 \times 3} & 0 \end{bmatrix}, \quad (32)$$

$$B_\sigma = \bar{B} := B_1, \quad (33)$$

where the correspondence between σ and σ_j , $j = 1, 2$, is given by Table I.

The objective function in (26) can be written as $(z - z^*)^T P(\bar{A}z + \bar{B} + \bar{A}_{1,\sigma_1} z_1 + \bar{A}_{2,\sigma_2} z_2)$. Minimizing this expression is equivalent to simultaneously solving the minimization problems:

$$\sigma_j(z) \in \arg \min_{m \in \mathcal{I}_2} (z - z^*)^T P \bar{A}_{j,m} z, \quad j = 1, 2, \quad (34)$$

which directly give the values σ_j corresponding to the state of each controlled switch S_j . Once again, the mode σ can be recovered by association of each pair (σ_1, σ_2) with each $\sigma \in \mathcal{I}_4$ (see Table I).

Now, consider (24) with P taking the following block-diagonal form:

$$P = \begin{bmatrix} P_1 & 0_{3 \times 3} & 0_{3 \times 1} \\ 0_{3 \times 3} & P_2 & 0_{3 \times 1} \\ 0_{1 \times 3} & 0_{1 \times 3} & p_3 \end{bmatrix}, \quad (35)$$

where $P_1, P_2 \in \mathbb{R}^{3 \times 3}$ and $p_3 \in \mathbb{R}$.

This choice for the form of P has been made so that switching law (26) can be used in such a way that the control signal for each converter depends only on its local variables. The zeroes in P are there to cancel the dependence of the control law on variables of the other converter or the DC bus. The LMI (24) can then be solved for the variables P_1, P_2 and p_3 . The solution of this problem is straightforward in commercial softwares such as MATLAB.

It can be shown that (34), with P taking the form (35), can be written as:

$$\sigma_j(z_j) \in \arg \min_{m \in \mathcal{I}_2} (z_j - z_j^*)^T P_j A_{j,m} z_j, \quad j = 1, 2. \quad (36)$$

Note that control law (36) can directly provide the gate signal for each converter j and only requires local measurements from each one. Moreover, since (36) has been derived from (26) with a matrix P that is a solution of (24), then the whole closed-loop system is globally exponentially stable.

Similarly to what has been done for a single converter, define $s_j(z_j) := (z_j - z_j^*)^T P_j D_j z_j$, where $D_j := A_{j,1} - A_{j,2}$, for $j = 1, 2$. The application of the ideal control law (36) for each converter j implies that:

- $\sigma_j(z_j) = 1$, if $s_j(z_j) < 0$;
- $\sigma_j(z_j) = 2$, if $s_j(z_j) > 0$;
- $\sigma_j(z_j) \in \{1, 2\}$, if $s_j(z_j) = 0$.

Therefore, the surface $s_j(z_j) = 0$ can be recognized as the switching surface corresponding to each converter j , and it only depends on the local variables z_j . Thus, by

defining parameters $h_j > 0$, $j = 1, 2$, hysteresis can be implemented for each converter in a similar fashion as it has been done for a single Boost converter in Section III-B.1. Under the assumption that h_j is sufficiently small and developing the equations for $|\dot{s}_j(z_j)|$ as in Section III-B.1, $f_{ss,j}$ is determined as:

$$f_{ss,j} = \frac{1}{2h_j} \frac{b_{j,1}^T P_j D_j z_j^* z_j^{*T} D_j^T P_j b_{j,2}}{\left(|b_{j,1}^T P_j D_j z_j^*| + |b_{j,2}^T P_j D_j z_j^*|\right)}, \quad j = 1, 2. \quad (37)$$

The acceptable current ripple for each converter (ΔI_j) is calculated in the same way as in (31). Thus:

$$\Delta I_j = \frac{\alpha_j^* E_j}{L_j f_{ss,j}}, \quad j = 1, 2. \quad (38)$$

Remark 2: Applying control law (36) with hysteresis boils down to comparing the absolute value of $s_j(z_j)$ (whose expression is simply given by a matrix product) with h_j , which can be advantageous in a real-time application. Moreover, P is computed offline. \square

IV. SIMULATION RESULTS

In this section, results from MATLAB simulations concerning the application of the methods developed in this paper are presented. In order to highlight their interest in the case of Boost converters, comparisons are made with current hysteresis control, briefly explained hereafter.

A. Current hysteresis control

Suppose that a certain current ripple ΔI is acceptable in the inductor of a single Boost converter. Then, *Current Hysteresis Control* (CHC) consists in the following:

- If the current $i(t)$ is lower than $i^* - \Delta I/2$, then activate mode 1;
- If the current $i(t)$ is higher than $i^* + \Delta I/2$, then activate mode 2;
- If $i(t)$ is in the hysteresis band defined by $|i(t) - i^*| \leq \Delta I/2$, then keep the same mode as before.

The use of CHC is widespread in the field of power electronics in general. Similarly to the technique discussed in this paper, CHC does not require a PWM module either. In the case of two converters, the procedure outlined above is carried out independently for each converter.

B. Single Boost converter

The parameters of the Boost converter represented in Fig. 1 are: $E = 400\text{V}$, $L = 1\text{mH}$, $C = 10\mu\text{F}$, and $R_o = 40\Omega$. The goal is to stabilize the voltage at $v^* = 600\text{V}$, which, from (5), corresponds to $1 - \alpha^* = E/v^* = 2/3$. From (7), $i^* = 22.5\text{A}$. The acceptable current ripple is taken to be $\Delta I = 5\text{A}$. From (30) and (31), $f_{ss} = 27\text{kHz}$ and $h = 19.8 \times 10^7$. Using MATLAB, matrix P is determined from (24) as $P = [\rho_1 \ \rho_2]$, with $\rho_1 = [11.6 \ -0.002]^T$ and $\rho_2 = [-0.002 \ 0.12]^T$.

Figs. 3 to 5 show a comparison of the results obtained from each method. Table II shows some performance indexes using both control techniques². It can be seen that the HBSC

²In this paper, the response time is considered to be the earliest time instant t_r such that the voltage remains bounded within $\pm 5\%$ around v^* for all $t \geq t_r$.

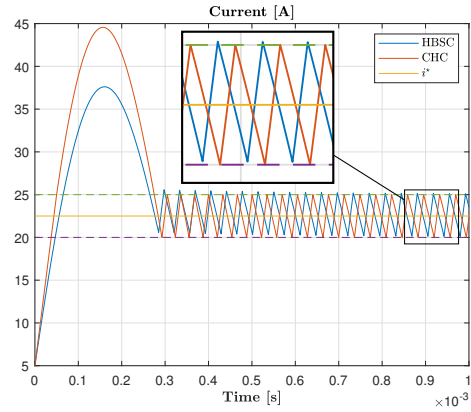


Fig. 3: Evolution of input current $i(t)$.

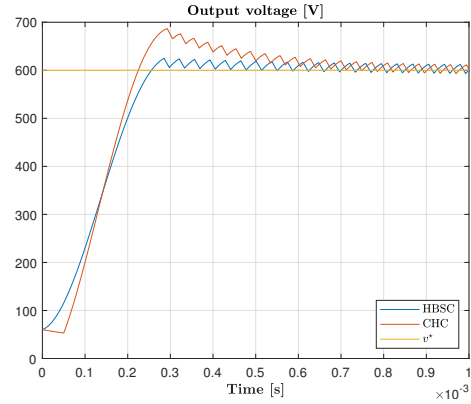


Fig. 4: Evolution of output voltage $v(t)$.

performed better in terms of current and voltage overshoot, as well as response time. Thus, the HBSC technique has brought improvements to the system response in transient behavior. Moreover, the steady-state behavior is the same using both methods. Indeed, it is shown in Fig. 3 that the current ripple is 5A in both cases. Fig. 5 shows the trajectory in state space using both methods.

C. Two Boost converters in parallel

The circuit parameters in Fig. 2 are the following: $E_1 = E_2 = 400\text{V}$, $L_1 = 10\text{mH}$, $L_2 = 8\text{mH}$, $L'_1 = 1\text{mH}$, $L'_2 =$

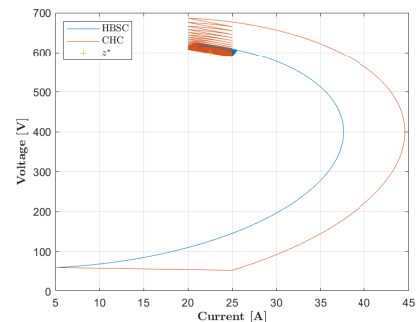


Fig. 5: System trajectory in the state space.

TABLE II: Performance indexes for the Boost converter.

	HBSC	CHC
Peak current (A)	37.6	44.6
Peak output voltage (V)	625	687
Response time (μ s)	235	558

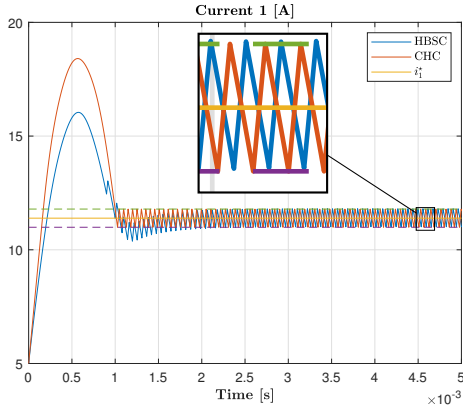


Fig. 6: Evolution of input current $i_1(t)$.

TABLE III: Performance indexes for the parallel connection of two Boost converters.

	HBSC	CHC
Peak current in conv. 1 (A)	16.0	18.4
Peak current in conv. 2 (A)	19.2	22.7
Peak output voltage (V)	615	689
Response time (μ s)	848	1801

0.6mH, $C_1 = C_o = 10\mu$ F, $C_2 = 15\mu$ F, $R'_1 = R'_2 = 1\Omega$, and $R_o = 40\Omega$. Here, the goal is also to stabilize the output voltage at $v^* = 600$ V. Assume that the load current should be equally shared between both converters, leading to $\kappa = 1$. From (19)-(23), $\alpha_1^* = \alpha_2^* = 0.34$. A matrix P in the form (35) that solves (24) is obtained. P_1 , P_2 and p_3 are given as:

$$P_1 = \begin{bmatrix} 12.4 & -0.004 & -0.040 \\ -0.004 & 0.013 & -0.011 \\ -0.010 & -0.011 & 1.25 \end{bmatrix}, \quad (39)$$

$$P_2 = \begin{bmatrix} 10.2 & -0.007 & -0.028 \\ -0.007 & 0.019 & -0.016 \\ -0.028 & -0.016 & 0.75 \end{bmatrix}, \quad (40)$$

and $p_3 = 0.013$. The acceptable current ripples are chosen to be $\Delta I_1 = 0.8$ A and $\Delta I_2 = 1.5$ A, corresponding to $h_1 = 3.0 \times 10^5$ and $h_2 = 5.2 \times 10^5$, according to (38). The steady-state switching frequencies are $f_{ss,1} = 17$ kHz and $f_{ss,2} = 11.4$ kHz. Figs. 6 and 7 show the plots obtained for $i_1(t)$ and $v(t)$, respectively. Current $i_2(t)$ is not shown due to lack of space, but its evolution is qualitatively similar to $i_1(t)$. Table III shows some performance indexes in this case. Note that the performance improvements seen in the case of a single converter have also been observed for the parallel association. Once again, the overshoots are smaller using the HBSC and the response time of the output voltage is faster.

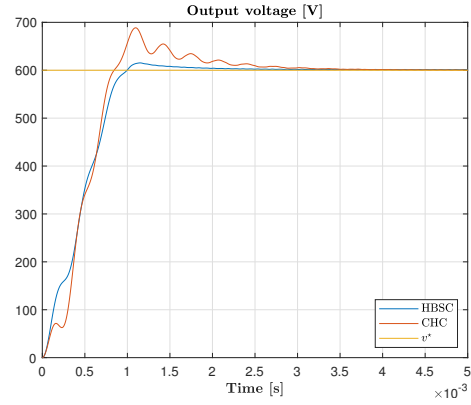


Fig. 7: Evolution of the DC bus voltage $v(t)$.

V. CONCLUSIONS AND FUTURE WORKS

In this paper, a control law that is well known in the switched systems literature has been adapted to include an hysteretic behavior, thus preventing unacceptable rises of the switching frequency. This control law has been applied to Boost converters and to their parallel interconnection. It has been shown that the switching frequencies can be easily chosen through the choice of the hysteresis parameters. In simulations where a comparison is established with a classical method that does not require PWM modulation either, the method presented in this paper has performed better as far as the transient behavior is concerned. Indeed, it can be seen in Tables II and III that the response time and the peak values are more satisfactory using this method. The steady-state behavior has been shown to be similar to the more traditional method. In addition, the gate signal to be selected at the current time step is determined only from local measurements and from the signal that had been formerly selected. The next step in this research is to verify the results in practice on an experimental setup.

REFERENCES

- [1] T. Dragičević, X. Lu, J. C. Vasquez, and J. M. Guerrero, "Dc microgrids—part I: A review of control strategies and stabilization techniques," *IEEE Transactions on Power Electronics*, vol. 31, no. 7, pp. 4876–4891, 2016.
- [2] W. Li and X. He, "Review of nonisolated high-step-up dc/dc converters in photovoltaic grid-connected applications," *IEEE Transactions on Industrial Electronics*, vol. 58, no. 4, pp. 1239–1250, 2011.
- [3] Z. Fusheng and R. Naayagi, "Power converters for dc microgrids—modelling and simulation," in *2018 IEEE Innovative Smart Grid Technologies-Asia (ISGT Asia)*, Singapore, 2018, pp. 994–999.
- [4] P. Bolzern and W. Spinelli, "Quadratic stabilization of a switched affine system about a nonequilibrium point," in *Proceedings of the 2004 American Control Conference*, Boston, MA, USA, 2004, pp. 3890–3895.
- [5] G. S. Deaecto, J. C. Geromel, F. S. Garcia, and J. A. Pomilio, "Switched affine systems control design with application to dc–dc converters," *IET Control Theory & Applications*, vol. 4, no. 7, pp. 1201–1210, 2010.
- [6] C. Albea-Sanchez, G. Garcia, S. Hadjeras, W. Heemels, and L. Zaccarian, "Practical stabilization of switched affine systems with dwell-time guarantees," *IEEE Transactions on Automatic Control*, vol. 64, no. 11, pp. 4811–4817, 2019.
- [7] Z. Kader, "Control and observation of switched affine systems," Ph.D. dissertation, Université Lille 1-Sciences et Technologies, 2017.
- [8] R. W. Erickson and D. Maksimovic, *Fundamentals of power electronics*. Springer Science & Business Media, 2007.